

CHAPTER 1

INTRODUCTION

1.1 Background of Study

Friction-stir welding (FSW) is a solid-state joining process (meaning the metal is not melted during the process) and is used for applications where the original metal characteristics must remain unchanged as far as possible. This process is primarily used on aluminum, and most often on large pieces which cannot be easily heat treated post weld to recover temper characteristics. It was invented and experimentally proven by Wayne Thomas and a team of his colleagues at The Welding Institute UK in December 1991 [1]. Figure 1 show how FSW is carried out by moving one component relative to the other along a common interface, while applying a compressive force across the joint. A cylindrical-shouldered tool with a profiled pin is rotated at a constant speed and fed at a constant traverse rate into the joint line between two pieces of sheet or plate material, which are butted together. The length of the pin is slightly less than the weld depth required and the tool shoulder should be in intimate contact with the work surface.

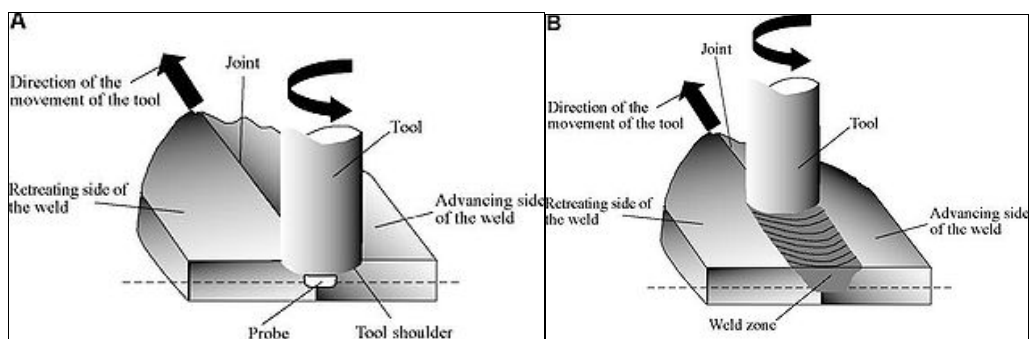


Figure 1: (A) Two discrete metal workpieces butted together, along with the tool (with a probe). (B) The progress of the tool through the joint, also showing the weld zone and the region affected by the tool shoulder.

[Source: http://en.wikipedia.org/wiki/Friction_stir_welding]

As the pin is moved in the direction of welding, the leading face of the pin, assisted by a special pin profile, forces plasticized material to the back of the pin while applying a substantial forging force to consolidate the weld metal.

The friction heating generated at the interface softens both components, along with the heat generated by the mechanical mixing process and the adiabatic heat within the material, cause the stirred materials to soften without reaching the melting point (hence cited a solid-state process), allowing the traversing of the tool along the weld line in a plasticized tubular shaft of metal and when they become plasticised the interface material is extruded out of the edges of the joint so that clean material from each component is left along the original interface. The relative motion is then stopped, and a higher final compressive force may be applied before the joint is allowed to cool. The key to friction welding is that no molten material is generated, the weld being formed in the solid state. The welding of the material is facilitated by severe plastic deformation in the solid state, involving dynamic recrystallization of the base material [2].

A number of potential advantages of FSW over conventional fusion-welding processes have been identified:

- Good mechanical properties in the as welded condition
- Improved safety due to the absence of toxic fumes or the spatter of molten material
- No consumables – conventional steel tools can weld over 1000m of aluminum and no filler or gas shield is required for aluminum
- Easily automated on simple milling machines – lower setup cost and less training
- Generally good weld appearance and minimal thickness under/over-matching, thus reducing the need for expensive machining after welding
- Low environmental impact

However, there are also some limitations of the process:

- Exit hole left when tool is withdrawn
- Large down forces required with heavy-duty clamping necessary to hold the plates together
- Less flexible than manual and arc processes (difficulties with thickness variations and non-linear welds)
- Often slower traverse rate than some fusion welding techniques although this may be offset if fewer welding passes are required.

1.2 Problem Statement

FSW has already been implemented extensively in Europe, America and Japan. However, this technology is still considered as a new technology in Malaysia; and it can be applied towards various industries including marine, automotive, and aerospace and also the oil and gas industries.

Based on the earlier research, implementation of FWS of the same material (Aluminum alloys) in Malaysia has yet to proceed although the knowledge is there for all to know. The sectors in the industrial settings might find such FWS process unproven in the Malaysia's industrial frame due to the lack of data and research in terms of the weld quality and properties of FSW [3].

FSW is energy efficient, environment friendly, and versatile. In particular, it can be used to join high-strength aerospace aluminum alloys and other metallic alloys that are hard to weld by conventional fusion welding. Using the GMAW (gas metal arc welding) to weld aluminum alloy takes a lot of time for the base-metal preparation [4]. Particular emphasis by FSW has been given to: (a) mechanisms responsible for the formation of welds and microstructural refinement, and (b) effects of FSW parameters on resultant microstructure and final mechanical properties.

A benefit of FSW is that it has significantly fewer process elements to control. In a fusion weld, there are many process factors that must be controlled—such as purge gas,

voltage and amperage, wire feed, travel speed, shield gas, arc gap. However, in FSW there are only three process variables to control: rotation speed, travel speed and pressure, all of which are easily controlled. The increase in joint strength combined with the reduction in process variability provides for an increased safety margin and high degree of reliability.

1.3 Objective

The objective of the project is:

1. To study the difference of the welded region occurred within the 6061-T6 Aluminum alloys when they undergo the FSW process.
2. To study the effect of rotational and traverse rate against the hardness of the welded region.

1.4 Scope of Study

This research focuses on 6061-T6 aluminum alloy, the microstructure developed by the FSW process and tool steel H13. 6061 is a precipitation hardening aluminum alloy, containing magnesium and silicon as its major alloying elements [6] that are much lighter and more corrosion resistant than plain carbon steel, but not as corrosion resistant as pure aluminum [5]. Figure 2 show tool steel H13 that refers to a variety of carbon and alloy steels that are particularly well-suited to be made into tools [3]. Their suitability comes from their distinctive hardness, resistance to abrasion, their ability to hold a cutting edge, and/or their resistance to deformation at elevated temperatures (red-hardness). H-grade tool steels were developed for strength and hardness during prolonged exposure to elevated temperatures. All of these tool steels use a substantial amount of carbide forming alloys. H1 to H19 are based on chromium content of 5%; H20 to H39 are based on a tungsten content of 9%-18% and chromium content of 3%-4%; H40 to H59 are molybdenum based [8]. Table 1 show the chemical compositions of tool steel H13. As for the development of microstructural features within FSW, the

solid-state nature of the FSW process is combined with its unusual tool and asymmetric nature, results in a highly characteristic microstructure [9].

Table 1: Chemical compositions of the tool steel H13

AISI NO	C,%	Mn,%	W,%	Si,%	Cr,%	Mo,%	V,%	Co,%
H13	0.35	0.40	-	1.0	5.0	1.5	1.0	-



Figure 2: Tool steel H13

[<http://qihui.win.mofcom.gov.cn/en/plate01/product.asp?id=70618>]

1.5 Relevancy and feasibility of project

The fabrication of the welding tool steel H13 is done by using CNC MAZAK Lathe turning machine at Building 16, Mechanical Engineering Department, UTP. Once the tool has been completely fabricated, it undergoes the heat treatment by using Box Furnace in Block 17. The CNC MAZAK milling machine is also used to run the FSW process onto the workpiece. The sample preparation for the study on the mechanical properties is done by using the abrasive cutter, mounting machine, grinding machine, polishing machine and etching reagent that are available in Building 17. In conclusion, all of the tools required to conduct FSW is available here in UTP.

CHAPTER 2

LITERATURE REVIEW

A three dimensional transient model with adaptive boundary condition between workpiece and backplate under the tool was developed in order to build qualitative frame work to understand the heat transfer process which could accurately model the heat transfer process in FSW of 2014-T6 Aluminum Alloy [10]. The calculated results were compared with experimental data published by researchers. The prediction showed that the maximum temperature gradients in longitudinal and lateral directions were located just beyond the shoulder edge. The difficulty of determining the temperature distribution near the moving pin has been reduced. This model can be used for coupled field analysis to model the coupled heat transfer process for tool and the workpiece during FSW. Using the numerically calculated temperature field, the residual stress in FSW plate can be determined.

A softened region composed of a weld and two HAZs, has clearly occurred in the FSW joints of the 2017-T351 Aluminum Alloy, thus the tensile properties of the joints are lower than those of the base material [11]. The welding parameters have significant effects on the tensile properties and fracture locations of the joints. When the revolutionary pitch is greater than a definite value, some void defects exist in the joints, the tensile properties of the joints are considerably low, and the joints are fractured at the weld center. When the revolutionary pitch is smaller than the definite value, no defects are formed in the joints, the tensile properties of the joints are at comparatively high levels and the joints are fractured near or at the interface between the weld nugget and the TMAZ on the advancing side.

Two locations have been identified for fatigue crack initiation: within the HAZ/TMAZ and over the weld nugget [12]. Crack initiation over the nugget region would appear to compromise fatigue life. Fatigue failure was influenced by the apparent flow features of the FSW process, with crack initiation within the weld region being related to the presence of macroscopic discontinuities in the flow pattern of the flow arm. Subsequent

crack propagation into the weld nugget was seen to follow the associated onion ring band structure. Differences in hardness between the bands have been identified, consistent with a mechanical contribution to crack deflection behavior.

Friction stir butt welds of 6082-T6 Aluminum Alloy plates were investigated [13]. The friction stir welded material revealed lower yield and ultimate stresses than the base material as well as lower elongation and hardness. For the monotonic tensile tests, failures occurred near the weld edge line. The fatigue crack growth behavior was characterized for different material locations from the friction stir weld, namely the base material, HAZ and friction stir material. An increase of the crack propagation resistance, i. e. lower crack propagation rates, was verified for the welded material in comparison with the HAZ or even the base material, which is consistent with a compressive residual stress field at the crack vicinity. SEM observations were performed for the three types of crack propagation paths illustrating the typical microstructures.

Friction stir butt welds of AA6082-T6 with AA6061-T6 were produced, as well as FS butt welds of each single alloy [14]. Microstructural changes induced by the friction stir welding process were clearly identified. Also, in the analysis of the dissimilar joint the mixture of the two alloys is easily identified by the different etching response of both alloys.

The microstructural and corrosion properties of friction stir welded 7075 Al Alloy were studied [15]. Considerable grain refinement in weld metal has been achieved and it may be due to frictional heating and plastic flow. Pitting corrosion resistance of weld metal is better than that of thermo-mechanical affected zone and the base metal.

Mechanical properties of FSW welded aluminum alloy 6082-T6 change within changing of process parameters [16]. Tensile strength of FSW welds is directly proportional to the travel/welding speed. Hardness drop was observed in the weld region. That softening was most evident in the heat affected zone on the advancing side of the welds that

corresponded to the failure location in tensile stress. An initial stage of a tunnel defect was found at the intersection of weld nugget and thermo-mechanically affected zone.

The effect of friction stir welding parameters on microstructure and mechanical properties of welds in 1mm thickness sheets of AA5182-H111 and AA6016-T4 automotive aluminum alloys was investigated. Welds were done in two series, using in each series different tool design and process parameters [17]. The welding parameters were selected in order to give colder welds in the second series than in the first series. The decrease in heat-input refined the microstructure of the nugget and increased the hardness of the thermo-mechanically affected zone of the welds in AA5182-H111, without reducing joint efficiency. On the contrary the welds of the second series in AA6061-T4 showed a reduction in hardness and joint efficiency. The tool with scrolled shoulder allowed reducing the tool tilt angle to zero and the prominence in the advancing side of the welds.

Microstructure is defined as the structure of a prepared surface or thin foil of material as revealed by a microscope above 25X magnification [18]. The microstructure of a material (of which we can broadly classify into metallic, polymeric, ceramic and composite) can strongly influence physical properties such as strength, toughness, ductility, hardness, corrosion resistance, high / low temperature behaviour, wear resistance, and so on, which in turn govern the application of these materials in industrial practice.

FSW produced in 1mm thick plates of AA 6016-T4 aluminum alloy, with two different tools, were analyzed and compared concerning the microstructure and mechanical properties [19]. For each tool, the welding parameters were optimized in order to achieve non-defective welds. The results obtained showed that the “hot” welds, obtained with the maximum tool rotational speed and the minimum traverse speed, have improved mechanical properties relative to the “cold” welds that were in undermatch condition relative to the base material.

FSW study represents the first-ever investigation of friction stir welds in a single crystal material, and is crucial for understanding the fundamental processes that occur during the process [20]. By “freezing in” the microstructure surrounding the welding tool, the team was able to determine the initial mechanism of texture evolution and grain boundary development that occur during FSW. The shear deformation generated by the welding process gradually rotates regions of the single crystal, which grow in size and misorientation as the welding deformation continues. This rotation continues until new grains achieve an easily-sheared orientation. Some regions of the weld may even rotate counter to the prevailing deformation field in order to achieve such an orientation. As the tool advances, the new grains gradually rotate to align with the deformation field. Further development of this grain structure and texture has been obscured by conventional recrystallization and severe deformation near the tool. Additional studies are required to determine the process of grain boundary evolution and texture evolution that occur after these initial stages.

FSW were produced in AA 5083 and AA 6082 aluminum using different combinations of plate thickness and welding speed [21]. The structure of FSW welds contains features that are not found in fusion welds. In a cross-section of welded joint, the central part has a shape of a “nugget”. Immediately adjacent to the nugget is the plastically-deformed and heat-affected so called “thermo-mechanically-affected-zone” which has only been affected by the heat flow [22]. The cross-sections show that the overall shape of the nugget is very variable, depending on the alloy used and the precise process conditions. It is found that two aluminum alloys can be friction stir welded if the welding parameters are carefully selected [23]. It is possible to perform dissimilar welding using different aluminum alloys. Research limitations are that the design of the welding probe which is used in the experiment is changed; the speed of the welding can be improved. The material of the welding probe can be changed.

An investigation has been carried out on the FSW of magnesium alloy, AM60 [24]. High pressure die casting samples have been butt-jointed at different rotational speeds and their mechanical properties of strength and strain were presented. FSW offers a

quality advantage that leads the welds strength and ductility. The microstructure and defect formation were conducted by optical and scanning electron microscopes. More attention was paid to failure mode of welded pieces near joined area or so-called thermo-mechanical affected zone under tension and voids formed during FSW. The effect of FSW processing parameters and casting thickness on the mechanical properties is presented.

Microstructure is defined as the structure of a prepared surface or thin foil of material as revealed by a microscope above 25X magnification [18]. The microstructure of a material (of which we can broadly classify to metallic, polymeric, ceramic and composite) can strongly influence physical properties such as strength, toughness, ductility, hardness, corrosion resistance, high/low temperature behavior, wear resistance, and so on, which in turn govern the application of these materials in industrial practice [25]. Microstructure can also refer to the microscopic description of the individual constituents of a material [24].

Grains are small crystals (crystallites) that form a three dimensional aggregate; they are normally viewed in sections, which by nature are limited to two dimensions. The main characteristics of a grain structure are the grain size, grain shape, and grain-shape anisotropy. The examples of the types of grain structure available include:

1. Impingent structure
2. Columnar structure
3. Equiaxed structure
4. Mature grain structure
5. Deformed grain structure
6. Inhibited recrystallization structure
7. Duplex grain structure

Grain size must be measured in three dimensions using standardized section planes, and required some auxiliary expression of grain shape. It is difficult to alter manufacturing

practices within normal limits such that reproducible, specified measurable grain size can be repeatedly obtained.

Equiaxed crystals are crystals that have axes of approximately the same length. Crystals of equal axial length have more planes on which to slip and thus have higher strength and ductility. Equiaxed grains can in some cases be an indication for recrystallization [26]. Measured grain sizes usually are expressed in the number of grains per square millimeter, mean area per grain, or mean diameter per grain [27]. The mean grain diameter is commonly used for cast alloys. Grain elongation or flattening may be expressed as a ratio of length to thickness, as observed in a longitudinal cross section.

Recrystallization is a process by which deformed grains are replaced by a new set of undeformed grains that nucleate and grow until the original grains have been entirely consumed [28]. Recrystallization is usually accompanied by a reduction in strength and hardness of a material and a simultaneous increase in the ductility. Thus, the process may be introduced as a deliberate step in metals processing or maybe an undesirable by product of another processing step. The most important industrial uses are the softening of metals previously hardened by cold work, which have lost their ductility and the control of the grain structure in the final product.

Based on the literature survey several research on FSW done onto aluminum alloys. The author has decided to go on the FSW process of 6061-T6 Aluminum alloys with the dimension of 100mm x 100mm x 10mm and study the effect of rotational and traverse speeds on the tensile strength of the welded region.

CHAPTER 3

METHODOLOGY

To achieve the objective of this project, there are many steps involved during the FSW operation and the preparation to examine the microstructure of the welded area.

3.1 Research methodology

Data gathering and research about tools and equipments and the investigations of the Friction Stir Welding (FSW) as the joining method are done. A thorough search will be made through the internet and from the libraries to collect all available information on FSW. The collections of technical details regarding tool fabrication and the important welding parameters. The results of the investigations and analysis will be objectively compared with the actual performance data.

3.2 Project activities

Reference from book, journal and magazine has been useful guideline in gathering information regarding proposed topic. Literature review has been done by referring all sources available. It also including revising all lab related lab work that need to be perform in the future finding. After all necessary information has been collected; it comes to part of fabricating the tool using lathe machine and using the tool to proceed with the FSW.

The project work flow starts with getting approval of the project by the supervisor and coordinator. Then the research and data gathering about the tools and equipment and the investigations of FSW is conducted. The project is later on continued by completing the scope of work that have been determined and is followed by updates. The Gantt charts for overall project activities are presented in Appendix 1 and Appendix 2.

The key milestones that have been achieved for FYP 1 are listed below:

1. Obtaining tool steel grade H13 for welding tool
2. Designing tool steel grade H13 using AutoCAD
3. Fabrication of welding tool grade H13 using the MAZAK Lathe Turning Machine
4. Applying heat treatment process onto the welding tool grade H13 using Box Furnace

The key milestones that will be achieved for FYP 2 are listed below:

1. Set up the welding tool onto the CNC MAZAK Milling machine together with computerized programming
2. Run the FSW process onto the work piece and applying different sets of parameters
3. Sample preparation for microscopic examination by applying the metallographic procedure
4. Perform microscopic examination using optical microscope
5. Study on mechanical properties using tensile test

3.3 Welding tool preparation

3.3.1 Research of tool steel H13 for welding tool

Tool steel refers to a variety of carbon and alloy steels that are particularly well-suited to be made into tools. The hardness, resistance to abrasion, ability to hold a cutting edge, and/or the resistance to deformation at elevated temperatures (red-hardness) are all the important characteristics of a tool steel. The welding tool for the FSW needs a special design in order to run onto the workpiece. For this project, the author decides to go with the basic design; compared to other models available in the industry.

3.3.2 Design and fabrication of tool steel H13

Figure 3 shows the CNC MAZAK Lathe Turning Machine that is used to fabricate the welding tool. Each welding tool for FSW has a shoulder whose rotation against the substrate generates most of the heat required for welding. The pin on the tool is plunged into the substrate and helps stir the metal in the solid state. The design of the tool is a critical factor as a good tool can improve the quality of the weld and the maximum possible welding speed. Tool material is desirably strong, tough and hard wearing at the welding temperature. The tool is first being designed by using AutoCAD (Appendix 3) and is then fabricated using CNC Lathe Turning Machine.



Figure 3: CNC MAZAK lathe turning machine

The tool's initial length is 70mm. The length of the shaft is 62mm and the pin length should be 80% of the workpiece; which is 8mm. the shaft is made long enough to attach the welding tool onto the CNC MAZAK milling machine. The shoulder diameter is designed to be 20mm while the pin diameter is 10mm. The welding tool has been fabricated using CNC MAZAK lathe turning machine based on the dimension designed. Next, the welding tool undergoes heat treatment using Box Furnace to alter its properties.

3.3.3 Hardness of tool steel H13 (before heat treatment)

Once the fabrication of the welding tool is done, its hardness is taken before it undergoes heat treatment; to prove that the hardness is increased after heat treatment. The hardness test is done using INDENTEC HARDNESS Testing Machine 9150 LKV as shown in Figure 4. The results are as shown in Table 2.

Table 2: Hardness of tool steel H13 before heat treatment

Readings	Rockwell Hardness
1	31.30
2	31.50
3	30.90
4	31.00
5	31.10
6	32.00
7	31.50
8	31.50
9	30.90
10	31.10
Total	312.80
Average	31.28

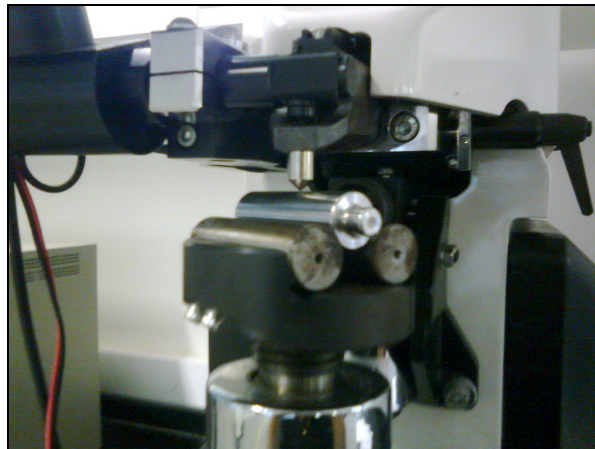


Figure 4: INDENTEC HARDNESS Testing Machine 9150 LKV

3.3.4 Heat treatment of tool steel H13

Heat treatment process is a method used to alter the physical and sometimes chemical properties of a material. The welding tool undergoes heat treatment using CARBOLITE Heat Treatment Furnace (Figure 5). Table 3 shows the procedures for the tool steel H13 heat treatment process.

Table 3: Heat treatment process

Process	Temperature (°C)	Time (hr)
Preheating	0 - 732	2
Preheating	732 - 760	2
Heating	1000	1
Cooling	30	2



Figure 5: CARBOLITE Heat Treatment Furnace

3.3.5 Hardness of tool steel H13 (after heat treatment)

Figure 6 shows the welding tool after it is being fabricated and after the heat treatment. The hardness is taken done the results is shown in Table 4.

Table 4: Hardness of tool steel H13 before heat treatment

Readings	Rockwell Hardness
1	42.2
2	56.1
3	44.9
4	40.4
5	40.3
6	44.4
7	52.0
8	49.4
9	51.6
10	42.7
Total	464
Average	46.4

The procedure is the same as in part 3.3.3.

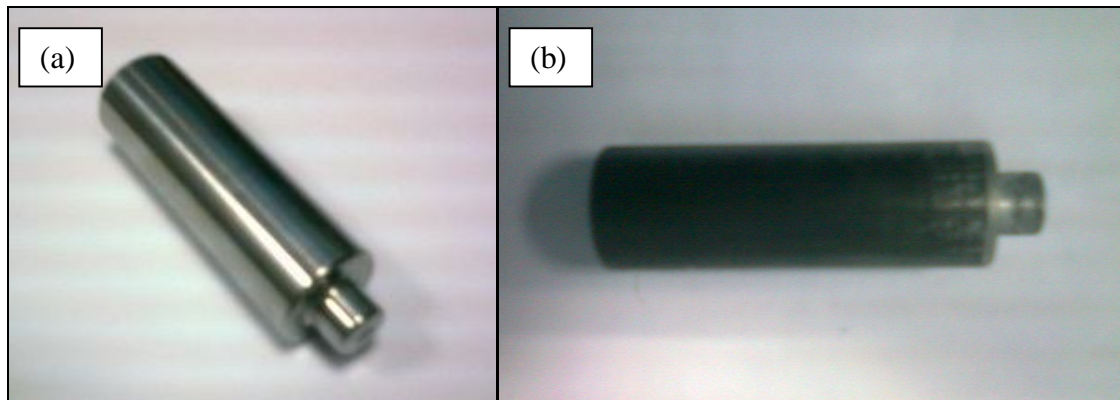


Figure 6: (a) Tool Steel H13 after being fabricated (b) Tool Steel H13 after heat treatment

3.4 Welding and experimental procedures

The work piece that is used in this project are 6061-T6 Aluminum alloys with the size of is 100mm x 100mm x 10mm each. Before the welding procedure started, the author need to drill two holes on each of the workpiece for the clamping arrangement as shown in Figure 7 (a). The dimension of the drilled hole is a diameter of 8.5mm holes for M10 x 1.5 specifications, together with thread for each hole. A few experimental runs of FSW will be made, altering each run with different rotational/spindle speed (N) in rpm and also the feed rate (S) in mm/min as shown in Table 5. Figure 7 (b) shows the CNC MAZAK Milling Machine that is used in joining the Aluminum alloys for the FSW process.

Table 5: Welding parameters for FSW

Run no.	Rotational speed (rpm)	Transverse speed (mm/min)	Depth of penetration (mm)	Length of weld line (mm)
1	2500	100	8.1	70
2	2500	15	8.1	70
3	2500	30	8.1	70
4	2000	30	8.1	70



Figure 7: (a) Drilling holes to the workpiece (b) CNC MAZAK Milling Machine

3.5 Sample preparation

To construct the microstructure examination, a sample preparation is needed. The metallographic preparation of aluminum alloys and magnesium alloys may vary considerably due to the wide range of chemical compositions and resulting hardness. Softer alloys generally are more difficult to be prepared by mechanical polishing because:

- Deformation caused by cutting and grinding extends to a greater depth.
- The embedding of abrasive particles in the metal during polishing is more likely.
- Relief between the matrix and second-phase particles, which are considerably harder than the matrix, develops more readily during polishing.

Thus, the sample presentation for this project consists of several processes to obtain microsections with smooth surface that are:

3.5.1 Sectioning

Sectioning is the removal of a conveniently sized and representative specimen from a larger piece. An abrasive non-ferrous cutter in Figure 8 (a) was used for sectioning part. The intended area to be examined is the welded area, thermo-mechanically affected zone (TMAZ), heat affected zone (HAZ) and the unaffected area. The cross section of sample will be taken for every zone of both materials.

3.5.2 Mounting

Mounting is necessary for subsequent handling and metallographic polishing. The Auto Mounting Press machine as shown in Figure 8 (b) is going to be used for this stage and a few parameters is involved in this process are the heating time and the cooling time. The samples that are going to be examined are mounted in a thermoset plastic material (BUEHLER Phenolic Powder Black).

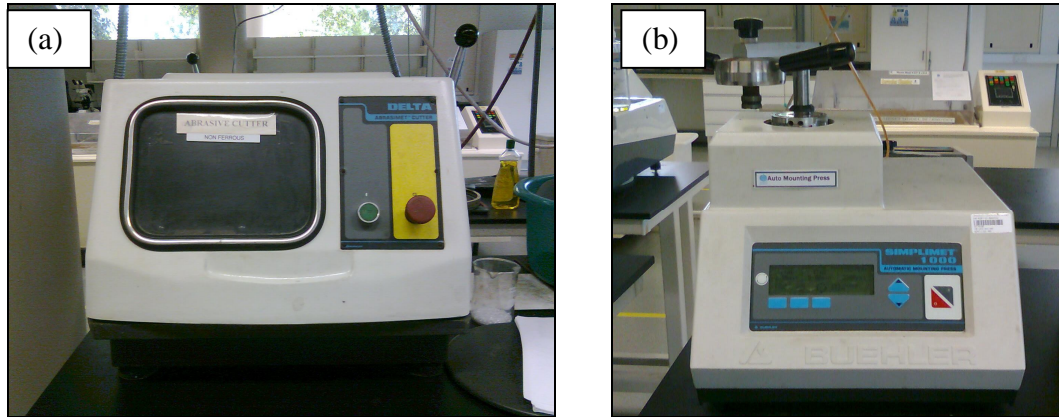


Figure 8: (a) Non-ferrous abrasive cutter (b) BUEHLER Auto Mounting Press machine

3.5.3 Grinding

MetaServ 2000 Grinder Machine (Figure 9) is used for this procedure. The useful abrasive of silicon carbide (SiC) is going to be used for the grinding process. Table 6 shows the procedure for grinding of the sample.



Figure 9: MetaServ 2000 Grinder machine

The main objectives of grinding are:

- To remove material deformed during cutting (rough, plane grinding)
- To remove the superficial layer of the specimen that covers the material destined for examination (rough, plane grinding)
- To prepare a flat surface while introducing only some residual or superficial deformation that can be eliminated during polishing (fine grinding)

Table 6: Procedure for fine grinding

Step	Abrasive	Gradation	Lubricant	Rotational Speed, rpm
1	SiC	120	H ₂ O	200
2	SiC	320	H ₂ O	200
3	SiC	400	H ₂ O	200
4	SiC	600	H ₂ O	200
5	SiC	1200	H ₂ O	200

3.5.4 Polishing

The main objective of polishing is to remove material deformation introduced by previous grinding and to obtain a flat, mirrorlike surface on a microscopic scale. The table below shows the procedure for polishing. Imptech 302 DVT Grinder Polisher Machine (Figure 10) is used for polishing procedure.



Figure 10: Imptech 302 DVT Grinder Polisher machine

3.5.5 Etching

The contrast between the microstructural constituents of a polished section can be improved by additional surface treatments such as chemical etching as it will deposit an interface layer of the specimen or sample. The main objectives of etching are:

- To attack and reveal the grain boundaries and the interface regions between the matrix and phase constituents.
- To cover the selected phase constituent surface with a thin film of chemical reaction products that improves or reveals the contrast between different structure components (visible in black-and-white mode).
- To cover the selected phase areas with a thin film of chemical reaction products that die/color the phase in a specific manner to allow phase identification (visible in color mode).

Aluminum alloys are very sensitive material and due to its nature of being ductile and soft, it is difficult to prepare by mechanical polishing. According to the ASM Handbook Volume 9, the suggested etching reagent and most widely used for Aluminum alloy is the Keller's reagent as indicated in Table 7.

Table 7: Recommended etching reagent to be used for aluminum alloys

Reagent name	Chemical composition	Etching mode	Application
Keller's reagent	100mL distilled H ₂ O 2.5mL HNO ₃ (70%) 1.5mL HCl (38%) 1.0mL HF (40%)	1-3 min	All kinds of Al alloys, reveals grain size, rolling direction, welding zone

3.6 Optical Microscope

The study of microstructural characteristic is going to be done with the help of optical microscope (Figure 11). Grain size and shape are the features to be study. Contrasts in the image produced results from differences in reflectivity of the various regions of the microstructure.

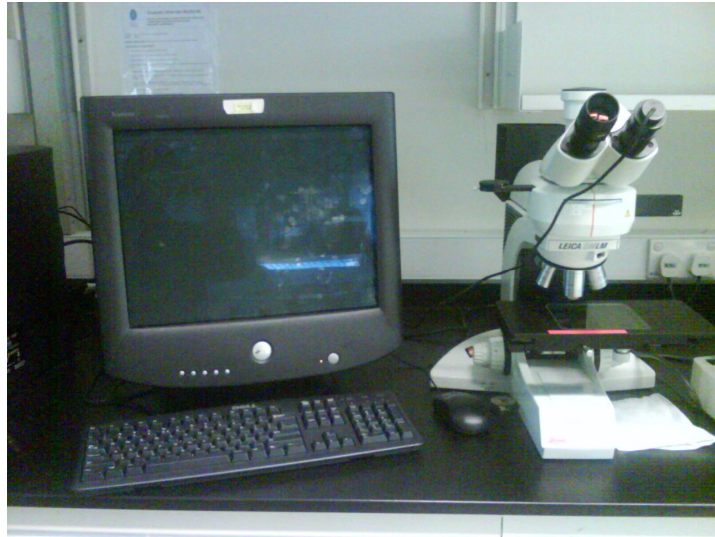


Figure 11: Optical microscope

3.7 Summary of methodology

Figure 12 shows the project work flow. The project is started by having the tool prepared by designing, fabricating and heat treatment. Next, the tool and the workpieces are set up in the CNC MAZAK Milling Machine for the welding procedure. After the welding is done, samples from the larger workpieces are taken by sectioning and are mounted so that it will be easier to handle. To properly examine the microstructure, the samples need grinding, polishing and etching. After the difference of the welded region is examined using optical microscope, hardness of the samples are taken to see the effects of the rotational and transverse speeds.

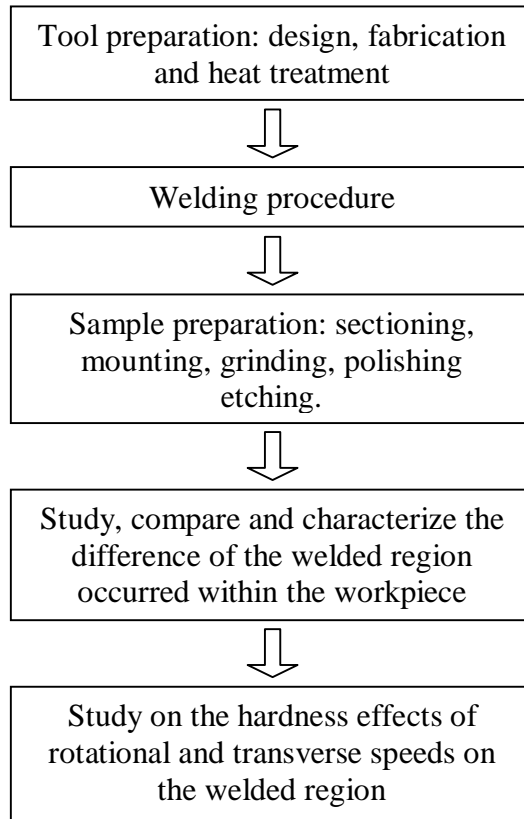


Figure 12: Project work flow

CHAPTER 4

RESULT AND DISCUSSION

First run is done onto a plate of aluminum alloys to test the weldability of the tool. Figure 13 shows the first run onto the aluminum plate without using the jig (Figure 14). From the result of the first run, it can be observed that there is big hollow on the front side of the welded area; while at the back side, the material shows a bulge. The welding process had not been facilitated with the addition of the jig which the function is to support the workpiece and gives better platform. Four holes were drilled in order to hold the workpiece in a better firm position and ensure the forces created by the welding tool does not spread and cause the final product to be oriented out of position.

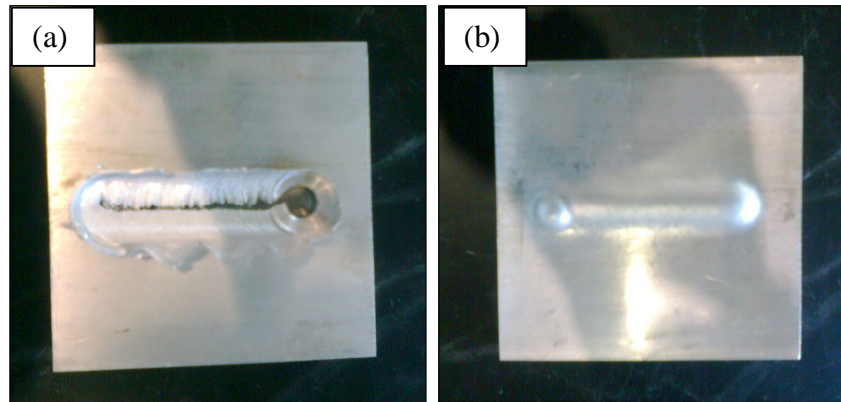


Figure 13: Run test result (a) front side view (b) back side view



Figure 14: The jig

Four pairs of 6061-T6 Aluminum Alloys with the dimensions of 100mm x 100mm x 10mm each were friction stir butt welded. The welding procedure is stated in Table 5.

From the optical microscopic examination, it can be observed that there is up to four different welded regions that are stir Nugget, thermo-mechanically affected zone (TMAZ), heat affected zone (HAZ) and base metal. Figure 15 shows the schematic diagram of microstructure characterizations for different welded region across FSW. The regions are classified based on the size of the grains developed after the FSW.

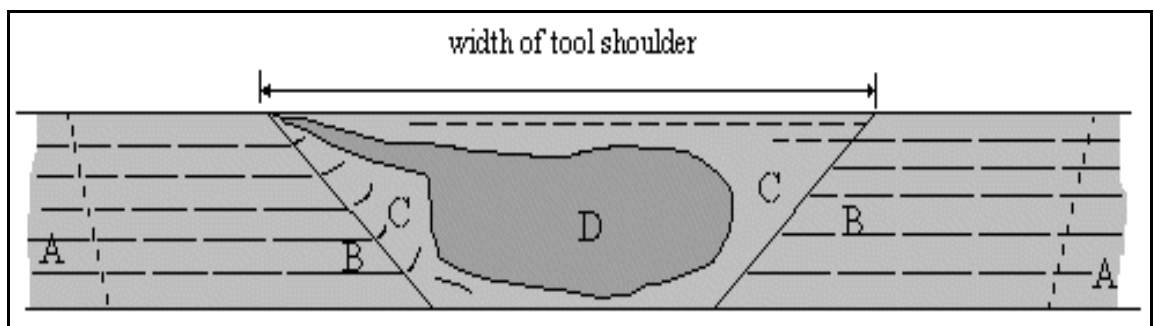


Figure 15: Schematic diagram of microstructure characterizations for different welded region across FSW

- A. Base metal
- B. Heat affected zone (HAZ)
- C. Thermo-mechanically affected zone (TMAZ)
- D. Stir nugget (SN)

Base metal: This part of the material is remote from the weld, which has not been deformed and which although it may have experienced a thermal cycle from the weld is not affected by the heat in terms of microstructure or mechanical properties.

Heat affected zone (HAZ): This region lies closer to the weld center. The material has experienced a thermal cycle which has modified the microstructure and/or the mechanical properties. The temperatures are lower than those in the TMAZ but may still have a significant effect if the microstructure is thermally unstable. There is no plastic

deformation occurring in this area. In age-hardened aluminum alloys this region commonly exhibits the poorest mechanical properties.

Thermo-mechanically affected zone (TMAZ): This region occurs on either side of the stir nugget. The strain and temperature are lower and the effect of the material has been plastically deformed by the FSW tool, and the heat from the process will also have exerted some influence on the material. The surrounding material that constraints the nugget metal is deformed by passage of the tool forms the remainder of the TMAZ and experiences much lower plastic strains ($\epsilon_{eff} \sim 0-5$) [30]. The primary cause of the softening at the TMAZ/HAZ boundary was determined due to coarsening and transformation of the strengthening precipitates during the welding process. Locations within the TMAZ achieve temperatures during welding that are sufficient to at least partially dissolve the precipitates.

Stir nugget (SN): The recrystallized area in the TMAZ in aluminum alloys has traditionally been called the nugget. Stir nugget is a region of heavily deformed material that roughly corresponds to the location of the pin during welding. The grains within the stir nugget are roughly equiaxed and often an order of magnitude smaller than the grains in the base material [9]. The microstructure here is determined by rubbing the rear face of the shoulder and the material may have been cooled below its maximum. It undergoes extreme levels of plastic deformation, reaching effective strains in excess of $\epsilon_{eff} \sim 40$ [30]; this normally leads to a very fine 2-10 μm recrystallized grain structure being formed in the center of the weld.

Figure 16 shows the cross section of the FSW plates. Plastic deformation (an irreversible change in the internal molecular structure by work and heat) occurs when large numbers of dislocations move and multiply. Generally, from the optical microscopic examination images taken (Figure 17 and 18) shows that the equiaxed grains of the microstructure of the stir nugget is by far the finest and smallest in terms of the shapes and size which is well defined due to its severe deformation affected by the dynamic recrystallization phenomena and the effect of thermal cycle within the 6061-T6 aluminum alloy. As it

heads towards the TMAZ, HAZ and base metal, the microstructure development goes bigger and coarser with respect to their shapes and sizes. With respect to the tunnel defect occurred within the welded region under the nugget zone, it is proved to have something to do with the design of the welding tool and also the variables or parameters of the welding process.

The generation of both at the advancing side and retreating side generates a non-balancing welding region in terms of generation of different welded region zone. This may be due to the downward forces exerted when the tool shoulder makes contact while it rotates counterclockwise during the welding operation. The metal on the advancing side is less affected much compared to the metal on the retreating side, indicating little impact on the rotating of welding tool. As it comes deeper inside, heading towards the stir Nugget (SN), the two other regions can be observed, which are the heat affected zone (HAZ) and thermo-mechanically affected zone (TMAZ).

There's also a difference between both the advancing side and retreating side which generates the HAZ and TMAZ region. When friction heat is generated, it forces the material to a softened condition without reaching its melting temperature point. Heat generation during FSW arises from two main sources that are the friction at the surface of the tool and the deformation of the material around the tool [29]. The heat generation is often assumed to occur predominantly under the shoulder, due to its greater surface area, and to be equal to the power required to overcome the contact forces between the tool and the workpiece.

Defect has also occurred within the sample which is referred to as tunnel defect or the 'worm-hole'. The size of the wormholes increases with the traverse speed [31] because of inadequate material flow towards the bottom of the weld. There are indications that the traverse speed to rotational speed ratio is an important variable in the formation of the tunnel defect [32]. For the same material and tool geometry, a high ratio tends to favor the formation of wormhole defects [33].

<p>Experiment 1</p> <p>Traverse rate : 2500 rpm Feed rate : 100 mm/min Depth of plunge: 8.1 mm Length of weld : 70 mm</p>	
<p>Experiment 2</p> <p>Traverse rate : 2500 rpm Feed rate : 30 mm/min Depth of plunge : 8.1 mm Length of weld : 70 mm</p>	
<p>Experiment 3</p> <p>Traverse rate : 2500 rpm Feed rate : 15 mm/min Depth of plunge : 8.1 mm Length of weld : 70 mm</p>	
<p>Experiment 4</p> <p>Traverse rate : 2000 rpm Feed rate : 30 mm/min Depth of plunge : 8.1 mm Length of weld : 70 mm</p>	

Figure 16: Cross section of friction stir welded plates

In the case of FSW, the grains of the welded region had been refined when the welded plates were exposed to work and heat which alters its hardness. When the grains are refined, magnesium component of the 6061-T6 Al alloys which create the grain boundary and hold the grains together increases. This makes the hardness of the welded region increases as it approaches the weld line. Figure 19 shows where the hardness tests have been taken.

Table 8 shows the HRF Hardness for the welded samples. For the fixed rotational speed of 2500 rpm and varied transverse speed; based on Figure 24, the transverse speed of 30 mm/min exhibits the highest in HRF hardness, the transverse speed of 15 mm/min and lastly the transverse speed of 100 mm/min. For the fixed transverse speed of 30 mm/min and varied rotational speed; based on Figure 25, the 2500 rpm rotational speed exhibits higher hardness than the rotational speed of 2000 rpm. All experiments show the increase of hardness compared to the base metal. The HRF Hardness from Table 8 is put in Figure 20 and 21 for better visual difference of the hardness.

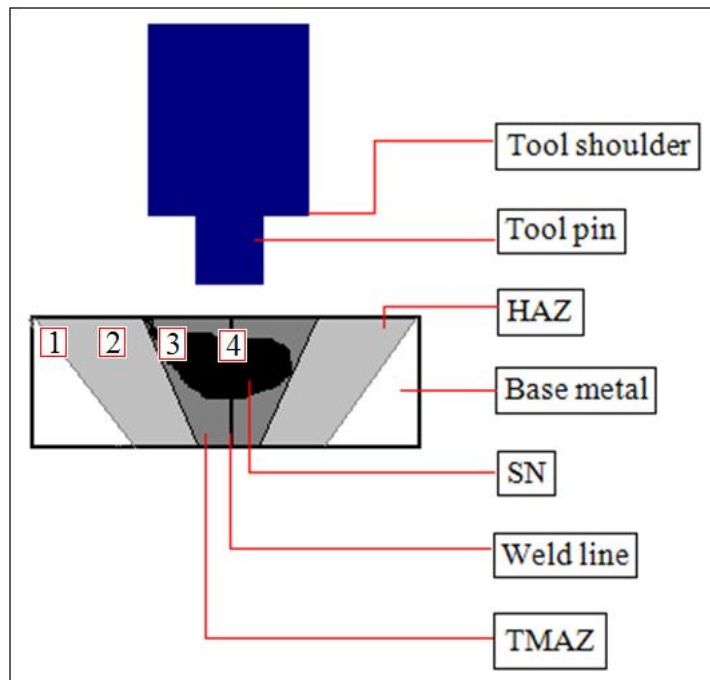


Figure 19: The point of HRF Hardness test

Table 8: HRF Hardness for welded samples

Reading	HRF (Base metal)	Experiment 1 HRF (2500rpm, 100mm/min)	Experiment 2 HRF (2500rpm, 15mm/min)	Experiment 3 HRF (2500rpm, 30mm/min)	Experiment 4 HRF (2000rpm, 30mm/min)
1	47.5	49.8	60.1	65.3	62.4
2	46.8	50.7	62.1	65.7	57.9
3	49.8	52.9	62.4	66.1	59.6
4	48.3	53.1	64.3	72.3	61.8

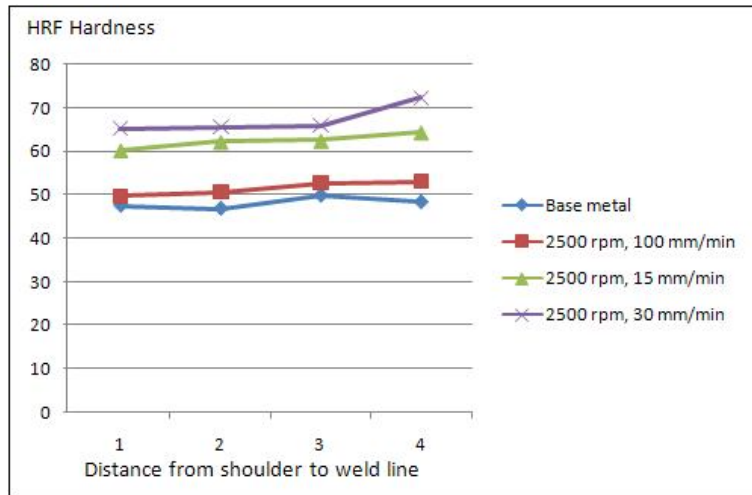


Figure 20: HRF hardness comparison for fixed rotational speed of 2500 rpm and varied traverse speed

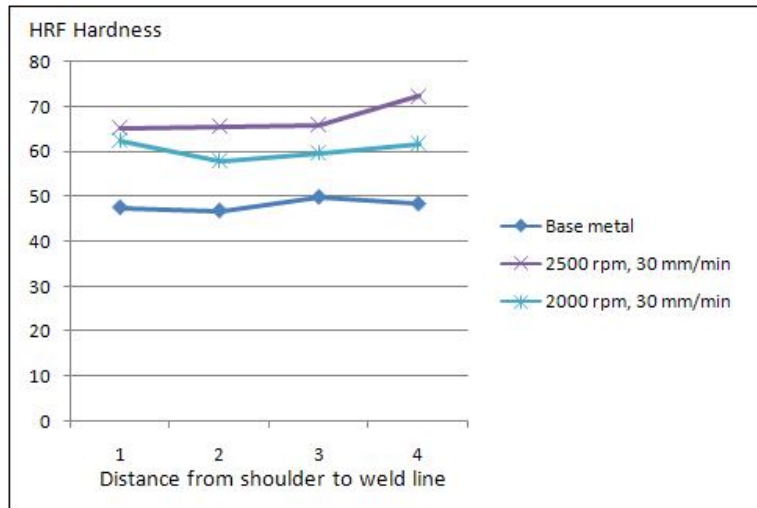


Figure 21: HRF hardness comparison for fixed traverse speed of 30 mm/min and varied rotational speed

CHAPTER 5

CONCLUSION AND RECOMMENDATIONS

The project is understood to achieve the objectives in studying the microstructure for different friction stir welded region of 6061-T6 aluminum alloy with different parameters and to study the effect of rotational and traverse rate against the hardness of the welded region. It can be agreed that there are four different regions appear across the cross section of the welded sample which are the friction stir processed zone or stir nugget (SN), thermo-mechanically affected zone (TMAZ), heat affected zone (HAZ) and base metal.

The images taken shows that the equiaxed grains of the microstructure of the stir nugget is by far the finest and smallest in terms of the shapes and size which is well defined due to its severe deformation affected by the dynamic recrystallization phenomena and the effect of thermal cycle within the 6061-T6 aluminum alloy. As it heads towards the TMAZ, HAZ and base metal, the microstructure development goes bigger and coarser with respect to their shapes and sizes. Defect has also occurred within the sample which is referred to as tunnel defect or the 'worm-hole'. A high ratio tends to favor the formation of wormhole defects [33]. With respect to the tunnel defect occurred within the welded region under the nugget zone, it is proved to have something to do with the design of the welding tool and also the variables or parameters of the welding process.

The hardness of the welded region increases as it approaches the weld line because of the grain refinement of the welded region. The grains of the welded region had been refined when the welded plates were exposed to work and heat which alters its hardness. When the grains are refined, magnesium component of the 6061-T6 Al alloys which create the grain boundary and hold the grains together increases. This makes the hardness of the welded region increases as it approaches the weld line. For the fixed rotational speed of 2500 rpm and varied transverse speed; the transverse speed of 30 mm/min exhibits the highest in HRF hardness, the transverse speed of 15 mm/min and lastly the transverse speed of 100 mm/min. For the fixed transverse speed of 30 mm/min and varied rotational speed, the 2500 rpm rotational speed exhibits higher hardness than the

rotational speed of 2000 rpm. All experiments however show the increase of hardness compared to the base metal.

With regards to the project work being carried out, there are recommendations that can be made that are:

- To have a wider range of proper aluminum alloy at disposal in experimenting the FSW process could embark more research and findings.
- To study the effect of other wide range of parameters to get better result.
- To study the effect of different design of welding tool of FSW on the welded quality and defects.
- To look into the outcome of FSW on dissimilar metals.

REFERENCES

1. Thomas, WM; Nicholas, ED; Needham, JC; Murch, MG; Temple-Smith, P; Dawes, CJ. Friction-stir butt welding, GB Patent No. 9125978.8, International patent application No. PCT/GB92/02203, (1991)
2. Ding, Jeff; Bob Carter, Kirby Lawless, Dr. Arthur Nunes, Carolyn Russell, Michael Suites, Dr. Judy Schneider (2008-02-14). "A Decade of Friction Stir Welding R&D At NASA's Marshall Space Flight Center And a Glance into the Future". NASA. Retrieved on 2009-04-14
3. Mohd 'Arriffuddin bin 'Allauddin; May 2009. An experimental study on microstructure of Friction Stir Welded plates
4. <http://www.lincolnelectric.com/knowledge/articles/content/alum.asp>
5. SAE aluminium specifications list, accessed Oct 8, 2006. Also SAE Aerospace Council, accessed Oct 8, 2006.
6. http://en.wikipedia.org/wiki/6061_aluminium_alloy
7. William D. Callister, Material Science and Engineering, 7th Edition
8. <http://en.wikipedia.org/wiki/H13>
9. Murr, LE; Liu, G; McClure, JC (1997). "Dynamic recrystallisation in the friction-stir welding of aluminium alloy 1100". *Journal of Materials Science Letters* **16** (22): 1801–1803. doi:10.1023/A:1018556332357
10. N. Rajamanickam, V. Balusamy. "Numerical Simulation of Transient Temperature in Friction Stir Welding of Aluminum Alloy 2014-T6"
11. H. J. Liu, H. Fujii, M. Maeda, K. Nogi. "Tensile Properties and Fracture Locations of Friction Stir Welded Joints of 2017-T351 Aluminum Alloy"
12. D. Booth, I. Sinclair. "Fatigue of Friction Stir Welded 2024-T351 Aluminum Alloy"
13. Moreira, P.M.G.P.; Jesus, A.M.P; Ribeiro, A.S. ; Castro, P.M.S.T.. "Fatigue Crack Growth Behavior of the Friction Stir Welded 6082-T6 Alumium Alloy"
14. P.M.G.P Moreira, T. Santos, S.M.O. Tavares, V. Richter-Trummer, P. Vilaca, P.M.S.T de Castro. "Mechanical and Metallurgical Characterization of Friction Stir Welding joints of AA6061-T6 with AA6082-T6"

15. T. Venugopal, K. Srinivasa Rao and K. Prasad Rao. "Studies on Friction Stir Welded AA 7075 Aluminum Alloy"
16. J. Adamoski, M. Szkodo. "Friction Stir Welds (FSW) of Aluminum Alloy AW6082-T6"
17. A. Loureiro, R.M. Leal, C. Leitaó, D.M. Rodriguez, P. Vilaca. "Friction Stir Welding of Automotive Aluminum Alloys"
18. ASM Metals Handbook, Ninth Edition, v. 9, "Metallography and Microstructures," American Society for Metals, Metals Park, OH, 1985, p. 12.
19. D.M. Rogrigues, A. Louriero, C. Leitaó, R.M. Leal, B.M. Chaparro, P. Vilaca, "Materials and Design", Sept 9, 2008
20. R. W. Fonda, J.A. Wert, A.P. Reynolds, W. Tang, "Initial Microstructural Evolution during Friction Stir Welding"
21. H. Larsson, L.-E. Svensson, and L. Karlsson: Proc. Welding and Joining Science and Technology, Madrid, Spain, ASM, 10-12 March 1997
22. K.-E. Knipstrom, and B. Pekkari: Svetsaren Vol. 52, No 1-2, 1997, pp 49-52
23. M. Vural, A. Ogur, G. Cam, C. Ozarpa, "On the friction stir welding of aluminum alloys EN AW 2024-0 and EN AW 5754-H22", *Archives Of Material Science and Engineering*, January 2009
24. R. W. Fonda, J.A. Wert, A.P. Reynolds, W. Tang, "Initial Microstructural Evolution during Friction Stir Welding"
25. <http://en.wikipedia.org/wiki/Microstructure>
26. According to Mabuchi, Yamada et al in "*The Grain size dependence of strength in the extruded AZ91 Mg alloy*", in "*Magnesium Alloys and their Applications*", edited by K.U. Kainer (2000), ISBN 3-527-30282-4
27. According to Mabuchi, Yamada et al in "*The Grain size dependence of strength in the extruded AZ91 Mg alloy*", in "*Magnesium Alloys and their Applications*", edited by K.U. Kainer (2000), ISBN 3-527-30282-4
28. According to Mabuchi, Yamada et al in "*The Grain size dependence of strength in the extruded AZ91 Mg alloy*", in "*Magnesium Alloys and their Applications*", edited by K.U. Kainer (2000), ISBN 3-527-30282-4

29. Qi, X, Chao, Y J (1999). “*Heat Transfer and Thermo-mechanical Analysis of FSW joining of 6061-T6 plates*”. *1st International Symposium in FSW (CD ROM), Thousand Oaks, USW: TWI*
30. Philip B. Prangnell, Chris P. Heason, Kevin J. Colligan. “Grain Structures in Al-alloy Friction Stir Welds Observed by Stop-Action Technique”
31. R. Crawford, G. E. Cook, A. M. Strauss, D. A. Hartman, and M. A. Stremmer. Experimental defect analysis and force prediction simulation of high weld pitch friction stir welding. *Science and Technology of Welding and Joining*, 11:657-665, 2006
32. H. J. Liu, H. Fujii, M. Maeda, and K. Nogi. *Tensile fracture location characterization of friction stir welded joints of different aluminum alloys. Journal of Materials Science and Technology*, 20:103-105, 2004
33. X. Long and S. K. Khanna. *Modeling of electrically enhanced friction stir welding process using finite element method. Science and Technology of Welding and Joining*, 10:482-487,2005